HUNGARIAN UNIVERSITY OF
AGRICULTURE AND LIFE SCIENCES

(SZENT ISTVÁN UNIVERSITY formerly)

Incorporation of phase change material into building envelope under hot location

DOI: 10.54598/003590

PhD Thesis

by

Qudama M. Q. Al-Yasiri

Gödöllő
2023

Doctoral school

Denomination: Doctoral School of Mechanical Engineering

Science: Mechanical Engineering

Leader: Prof. Dr. Gábor Kalácska, DSc
Institute of Technology
Hungarian University of Agriculture and Life Sciences,
Gödöllő, Hungary

Supervisor: Associate Prof. Dr. Márta Szabó, PhD
Institute of Technology
Hungarian University of Agriculture and Life Sciences,
Gödöllő, Hungary

…… ……

Affirmation of supervisor Affirmation of head of school

CONTENTS

1. INTRODUCTION, OBJECTIVES

Energy consumption in buildings has become an urgent issue in most countries worldwide. According to the International Energy Agency (IEA), the building sector is responsible for the highest share of total energy consumption worldwide by about 40%. Furthermore, this trend will continue, where the energy consumed for space heating and cooling is predicted to be high by up to 12% and 37%, respectively, in 2050.

Building envelope plays a predominant role in controlling building energy by adjusting the heating/cooling loads between the indoor and outdoor environments to satisfy the building's thermal requirements. The latest report of IEA stated that building construction and operations accounted for 36% of the final global energy used in buildings and 39% of the energy-related CO_2 emissions in 2018. Therefore, a good opportunity to increase building energy efficiency could be achieved through the building envelope.

Different solutions have been introduced to minimise the heating and cooling loads through building envelopes towards energy-efficient buildings. Amongst other successful strategies, incorporating phase change materials (PCMs) into building envelopes has proven to have the desired impact of controlling the thermal load, resulting in a remarkable energy saving. PCMs are implemented to minimise the building thermal load due to their massive energy storage potential during phase transition. This research area is still ongoing, and many questions are still open for discussion towards optimal thermal behaviour and the highest performance. Therefore, the detailed research objectives of this thesis are as follows:

- To investigate the optimal passive PCM layer position in composite roof construction compared to bare roof construction.
- To investigate the optimal passive PCM layer thickness within the composite roof construction.
- To examine the optimal integration of passive PCM capsules into constructive bricks.
- To quantify the thermal comfort and energy-saving of a scaled PCM room under no ventilation on an hourly, daily, and long-term basis.
- To study the role of thermal insulation when combined with a PCM room considering the optimal position and thickness of insulation concerning the PCM incorporated.
- To explore the effect of natural night ventilation through a single-side opening (window) on the PCM room thermal performance.

2. MATERIALS AND METHODS

This chapter covers the description of the materials, techniques, and equipment used, as well as the scientific methodologies employed in the experimental measurements to accomplish the research goals.

2.1. Description and experimental set-up

The experimental and numerical investigations have been confirmed under the subtropical desert climate of Al Amarah city (Latitude: 31.84°N and Longitude: 47.14°E), Maysan Province, southern Iraq. The experimental set-up comprised two scaled rooms; one was used as a reference and the other incorporated PCM into the roof and walls. Three follow-up experiments were conducted for PCM room construction to investigate the optimal PCM position and thickness within the roof and the best PCM-concrete brick.

The first experiment investigated the optimal position of a PCM layer within the roof, considering three different positions of the PCM layer within the roof combination. The traditional roof comprised three layers: Isogam as a roofing layer, concrete as a main layer and gypsum mortar as a cladding layer. Accordingly, a PCM layer of 1 cm was installed between the roofing and main layers, in the middle of the main layer and between the main layer and cladding layer. Two cases were studied in which one used the regular Isogam roofing layer (Case I), whereas the other used Isogam without a reflective layer (Case II). The second preliminary experiment investigated the optimal thickness of the PCM layer considering 1, 1.5 and 2 cm placed at the optimal position obtained in the first experiment.

The third experiment was conducted to specify the best thermally-enhanced concrete brick with PCM. Eight concrete bricks were fabricated with 23, 12, and 7 cm dimensions; one was left bare, and seven bricks contained PCM capsules of different shapes and sizes but with equal PCM quantity (~145 g).

Two scaled rooms of 1 m^3 were built and examined under severe hot summer days, comprised of thin roofs and walls and a small window fixed on the east wall. One room was assigned as a reference room for comparison, and the other was considered the best case obtained in the above preliminary experiments (PCM room). The PCM used is an Iraqi petroleum-based paraffin wax with a melting temperature range of 40 °C- 44 °C, suitable for the temperature variation in the location under study. The PCM was macroencapsulated inside galvanised steel panel to be used in the roof, while it was encapsulated inside aluminium containers for PCM-brick preparation (third experiment). Fig. 1 shows the final arrangement of rooms.

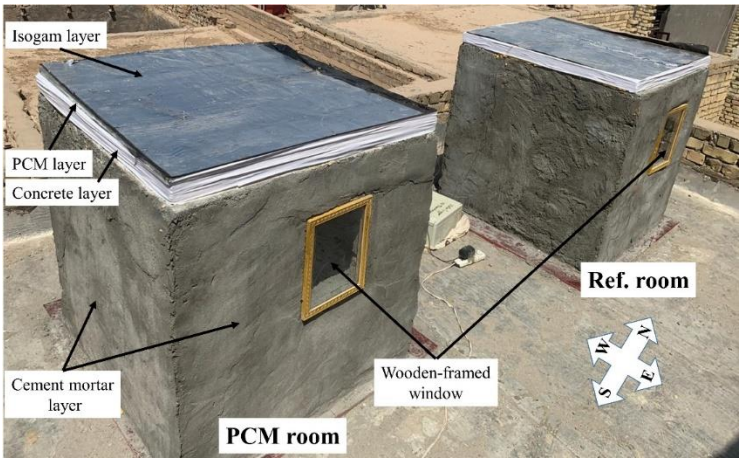

Fig. 1. 3D view of final experimental rooms

Table 1 shows the main characteristics of the PCM and construction materials.

Table 1. Materials used for experimental rooms' construction

Material	Thickness (cm)	k (W/m.K)	ρ (kg/m^3)	C_p (J/kg.K)
Isogam	0.4	0.35	1400	1100
Concrete layer	5	1.49	2300	800
Gypsum mortar	0.2	0.23	980	896
Cement mortar	1-2	0.99	2020	1000
Concrete brick	7	1.4	1440	750
Plywood	3	0.18	950	1200
Paraffin wax (PCM)	-----	0.21	930 (solid) 830 (liquid)	2100
Single glazing (window)	0.6	--------	--------	--------

2.2. Instrumentation

A multi-channel Arduino (type Mega 2560) based data logger was connected to T-type thermocouples with a temperature range of -270 °C to 370 °C and accuracy of ±0.5 °C) were used to measure the surface temperature of models/rooms in addition to the indoor and outdoor air temperatures. The data logger was programmed to measure and record temperatures every 10/30 min throughout the experiments and store data continuously in a portable micro storage memory connected to the Arduino.

On the other hand, a handy solar power meter (Type SM206 with a range of 0.1-399.9 W/m^2 and accuracy of ±10 W/m^2) was used to measure the incident solar radiation during the daytime. In addition, a thermal camera (model WB-80VOLTCRAFT®) of a temperature sensor ranging from -20 °C to 600 °C

with an accuracy of ±2% ±2 °C was used to show the temperature behaviour of outside surfaces temperature of models/bricks/rooms.

The best PCM brick attained in the third experiment and used later to construct the PCM room was tested at the age of 28 days using a compression test machine (ADR Touch head) to specify the mechanical strength declination.

2.3. Numerical formulation

Numerical studies were conducted to extend the results obtained in the experimental studies over the summer period. Besides, some other studies regarding the effect of natural night ventilation (NNV) and thermal insulation were not easy to attain experimentally. In this regard, a PCM room model was developed from the same construction materials used in the experimental studies. The room model was simulated using EnergyPlus software, the popular in building energy simulation studies.

The EnergyPlus can simulate buildings-based PCM via a one-dimensional conduction finite-difference solution algorithm to overcome the phase change phenomenon. In this regard, the PCM layer loaded into the building envelope is expressed using a fully-implicit first-order scheme according to Eq. (1).

$$\rho C_p \Delta x \frac{T_i^{j+1} - T_i^{j}}{\Delta t} = \left(k_W \frac{\left(T_{i+1}^{j+1} - T_i^{j+1}\right)}{\Delta x} + k_E \frac{\left(T_{i-1}^{j+1} - T_i^{j+1}\right)}{\Delta x} \right) \quad (1)$$

where ρ is the layer density (kg/m^3), C_p is the specific heat capacity (kJ/kg.K), Δx is the layer thickness (m), and Δt is the calculation time step (s). T is the node temperature (K), whereas i denotes the modelled node. Subsequently, $i+1$ and $i-1$ represent the adjacent nodes concerning the inner and outer sides, respectively. $j+1$ is the instant time step, whereas j is the previous time step. kW is the thermal conductivity of the interface between i and $i+1$ nodes, whereas kE is the thermal conductivity for the interface between the i and the $i-1$ nodes (W/m.K). k_W and k_E could be calculated by Eq.(2) and Eq.(3), as follows:

$$kw = \frac{\left(k_{i+1}^{j+1} + k_i^{j+1}\right)}{2} \quad (2)$$

$$k_E = \frac{\left(k_{i-1}^{j+1} + k_i^{j+1}\right)}{2} \quad (3)$$

Since the C_p of the PCM layer is a temperature-dependent property every time, its value could be calculated by Eq. (4) as follows:

$$C_p = \frac{h_i^{j} - h_i^{j-1}}{T_i^{j} - T_i^{j-1}} \quad (4)$$

The following assumptions were considered to simplify the transient simulation:

- The PCM and construction materials are homogeneous and isotropic, with no heat generation within the material.
- The PCM layer is in perfect contact with the roof and wall layers, and the contact resistance is negligible.
- The outer surface temperature of the room elements was calculated as a sol-air temperature ($T_{sol\text{-}air}$), according to Eq. (5).

$$T_{sol-air} = T_a + \frac{\alpha I_{inc}}{h_o} - 3.9°C \quad \text{for roof}$$
$$T_{sol-air} = T_a + \frac{\alpha I_{inc}}{h_o} \quad \text{for walls} \tag{5}$$

In some cases, exploring the PCM effectiveness within the element is necessary by considering the percentage of liquid and solid states. This can be attained by calculating the liquid fraction according to Eq. (6).

$$Liquid\ fraction = \begin{cases} 0 & \text{if } T_n \geq T_l \text{ (Solid phase)} \\ \dfrac{T - T_s}{T_l - T_s} & \text{if } T_l > T \geq T_s \text{ (Mushy zone)} \\ 1 & \text{if } T_n < T_s \text{(Melting phase)} \end{cases} \tag{6}$$

where T,T_l and Ts are the temperatures of the node, liquid and solid PCM.

2.4. Equations used to evaluate the thermal performance

Several energetic and thermal comfort indicators were analysed to show the improvement of the PCM element/room compared with the reference one considering the inner surface temperature (T_{in}), outer surface temperature (T_{out}), indoor temperature (T_i) and outdoor ambient temperature (T_o). These indicators are as follows:

Maximum temperature reduction (MTR)

MTR is the temperature reduction of the element surface temperature in the PCM room compared with the reference one, according to Eq. (7).

$$MTR = T_{out,max.} - T_{in,max.} \tag{7}$$

The same concept was followed in some cases to indicate the room maximum temperature reduction (RMTR), referring to the maximum reduction in the indoor room temperature according to Eq. (8), as follows:

$$RMTR = \frac{T_{i,max,reference} - T_{i,max,PCM}}{T_{i,max,reference}} \times 100\% \tag{8}$$

Decrement factor (DF)

The DF could be calculated according to Eq. (9).

$$DF = \frac{T_{in,max} - T_{in,min}}{T_{out,max} - T_{out,min}} \tag{9}$$

Time lag

The time lag (TL) of the element was calculated according to Eq. (10):

$$TL = \tau_{T_{in,max}} - \tau_{T_{out,max}} \quad (10)$$

where $\tau_{in,max}$ and $\tau_{out,max}$ are the time at the element's maximum T_{in} and T_{out}.

Average temperature fluctuation reduction (ATFR)

ATFR is the summation of the average decrease in the envelope temperature during the day (X) and the average increase in the envelope element temperature at night (Y), according to Eq. (11)-Eq. (13).

$$ATFR = X+Y \quad (11)$$

$$X = T_{\boldsymbol{in,av.,reference}} - T_{\boldsymbol{in,av.,PCM}} \quad (12)$$

$$Y = T_{\boldsymbol{in,av.,PCM}} - T_{\boldsymbol{in,av.,reference}} \quad (13)$$

Thermal load levelling (TLL)

The TLL inside investigated rooms was calculated using Eq. (14) and (15).

$$TLL_{Ref\ room} = \frac{T_{i,reference,max} - T_{i,reference,min}}{T_{i,reference,max} + T_{i,reference,min}} \quad (14)$$

$$TLL_{RCM\ room} = \frac{T_{i,PCM,max} - T_{i,PCM,min}}{T_{i,PCM,max} + T_{i,PCM,min}} \quad (15)$$

Operative temperature reduction (OTR)

The operative temperature (OT) was calculated as the average indoor air temperature and mean radiant temperature ($\bar{T}_{mr}$), according to Eq. (16).

$$OT = \frac{T_i + \bar{T}_{mr}}{2} \quad (16)$$

$\bar{T}_{mr}$ can be calculated considering the surface temperature and element area.

Accordingly, the OTR was calculated according to Eq. (17).

$$OTR = \frac{OT_{reference} - OT_{PCM}}{OT_{reference}} \times 100\% \quad (17)$$

Heat gain reduction (HGR)

The solar heat gain (HG) of each element in the reference and PCM room was calculated according to Eq. (18).

$$HG = h_i\ A\ (T_{in} - T_i) \quad (18)$$

Consequently, the HGR can be calculated considering the HG in each corresponding element of PCM and reference rooms, according to Eq. (19).

$$HGR = \frac{HG_{reference} - HG_{PCM}}{HG_{reference}} \times 100\% \quad (19)$$

3. RESULTS AND DISCUSSION

This chapter presents the most important results obtained from the experiments and numerical investigations and their discussions.

3.1. Investigation of the optimal PCM position within the roof

The experimental work to indicate the optimal PCM layer within the roof described in section 3.3.2 lasted for one week during August and September 2020. The measurements of Case I were collected for three consecutive days (29-31.08.2020), whereas Case II was conducted for four days from 11-14.09.2020. Fig. 2 shows the temperature profile as a function of time for Model A, Model B, Model C and Model D, respectively, in case II.

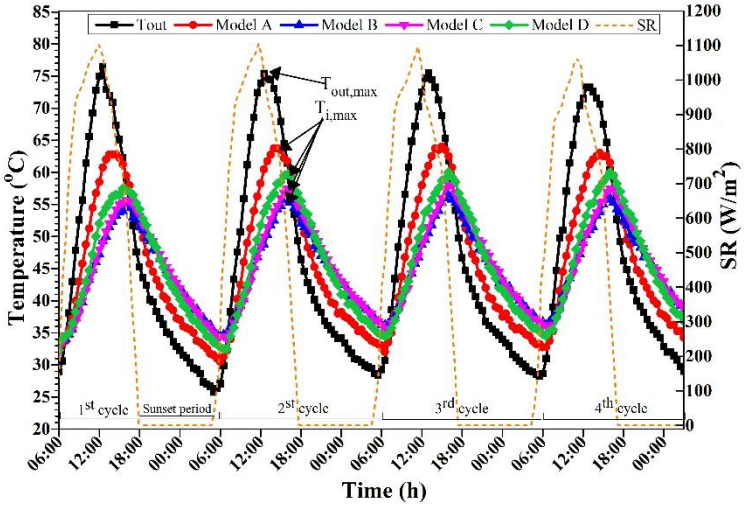

Fig. 2. Temperature profile for tested models (Case II)

As expected, it can be noticed that all models containing the PCM layer have better thermal performance than the reference case, thanks to the thermal storage potential of the PCM layer. Table 2 and Table 3 show a summary of obtained results in Case I and Case II, respectively.

Table 2. Summary of average results of indicators in Case I

Model	Average RMTR (%)	Average DF	Average TL (min)	Average ATFR (°C)
Model A	-----	0.78	-----	-----
Model B	8.6	0.53	126.7	6.6
Model C	7.3	0.53	113.3	7.3
Model D	4.6	0.60	86.7	5.3

Table 3. Summary of average results of indicators in Case II

Model	Average RMTR (%)	Average DF	Average TL (min)	Average ATFR (°C)
Model A	-----	0.82	-----	-----
Model B	12.1	0.47	152.5	8.8
Model C	9.8	0.49	152.5	8.8
Model D	6.4	0.59	122.5	6.3

3.2. Investigation of the optimal PCM layer thickness within the roof

The experiment to investigate the optimal PCM layer thickness presented in section 3.3.3 was conducted for three consecutive thermal cycles, from 3-5/9/2020. Fig. 3 shows the indoor temperature of PCM rooms (Model B, Model C and Model D) with different thicknesses than the reference room model (Model A).

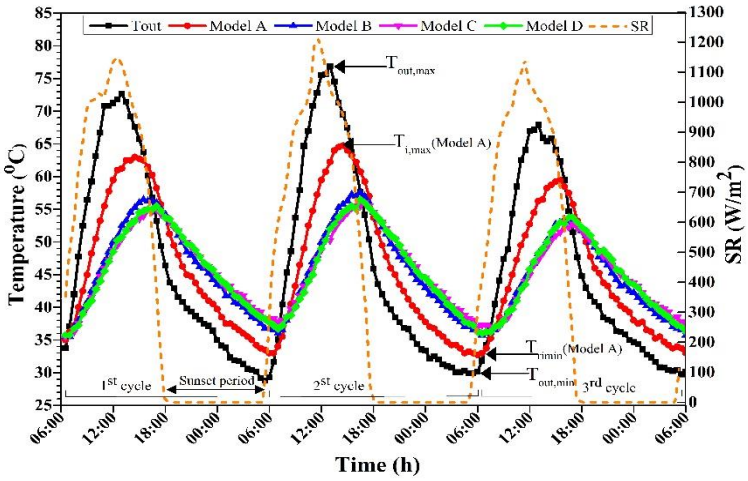

Fig. 3. T_i profile of experimental models

Due to PCM heat storage capacity, T_{in} and T_i in PCM models were generally lower than those of the reference model. In this regard, T_{in} and T_i decreased as the PCM layer's thickness increased, which shows the PCM's ability to shave temperature fluctuations during peak hours. Table 4 summarises the main results of this study.

Table 4. Summary of different PCM thicknesses results.

Model	Average RMTR (%)	Average DF	Average TL (min)	Average ATFR (°C)
Model A	-----	0.84	-----	-----
Model B	10.4	0.54	100.1	8.13
Model C	12.2	0.48	133.3	10.04
Model D	12.7	0.44	156.7	9.75

3.3. Investigation of the optimal PCM-incorporated concrete brick

This experimental work was conducted for four hot days, from 16.09.2020 to 6:00 of 20.09.2020. The measurements showed that maximum T_{in} during peak hours was reduced in all PCM bricks compared to the reference brick, as indicated in Fig. 4, showing a positive contribution of PCM to concrete bricks.

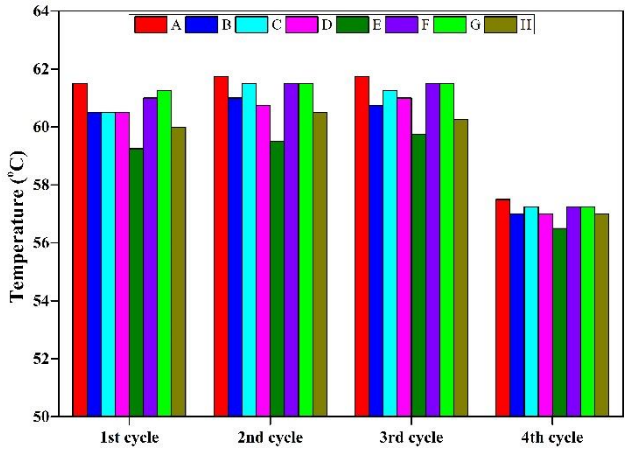

Fig. 4. Maximum T_{in} of tested concrete bricks at peak hours

The results of tested PCM concrete bricks considering all the above indicators are tabulated in Table 5.

Table 5. Summary of the experiment results

Brick sample	Overall heat transfer area (cm^2)	Average MTR (°C)	Average DF	Average TL (min)
B	529.9	0.8	0.903	35
C	196	0.5	0.932	37.5
D	224	0.8	0.917	40
E	320	1.9	0.901	42.5
F	300	0.3	0.937	40
G	310	0.3	0.923	40
H	348	1.2	0.910	42.5

3.4. Thermal performance of scaled experimental PCM room

This study has three concepts: one-day evaluation, hourly analysis and long-term investigation.

3.4.1. One-day assessment of PCM room thermal performance

This experiment was conducted for 24 h on 16th September 2021. The recorded T_{in} and T_{out} for the roof and walls of PCM and reference rooms are shown in Fig. 5 . The outdoor temperature recorded a minimum of 30.5 °C in

the early morning and a maximum of 47.5 °C in the midday at 13:40. The maximum T_{out} reached 56.5 °C, 56 °C, 52.75 °C, 59.25 °C and 53.75 °C for the east wall, west wall, north wall, south wall and roof, respectively.

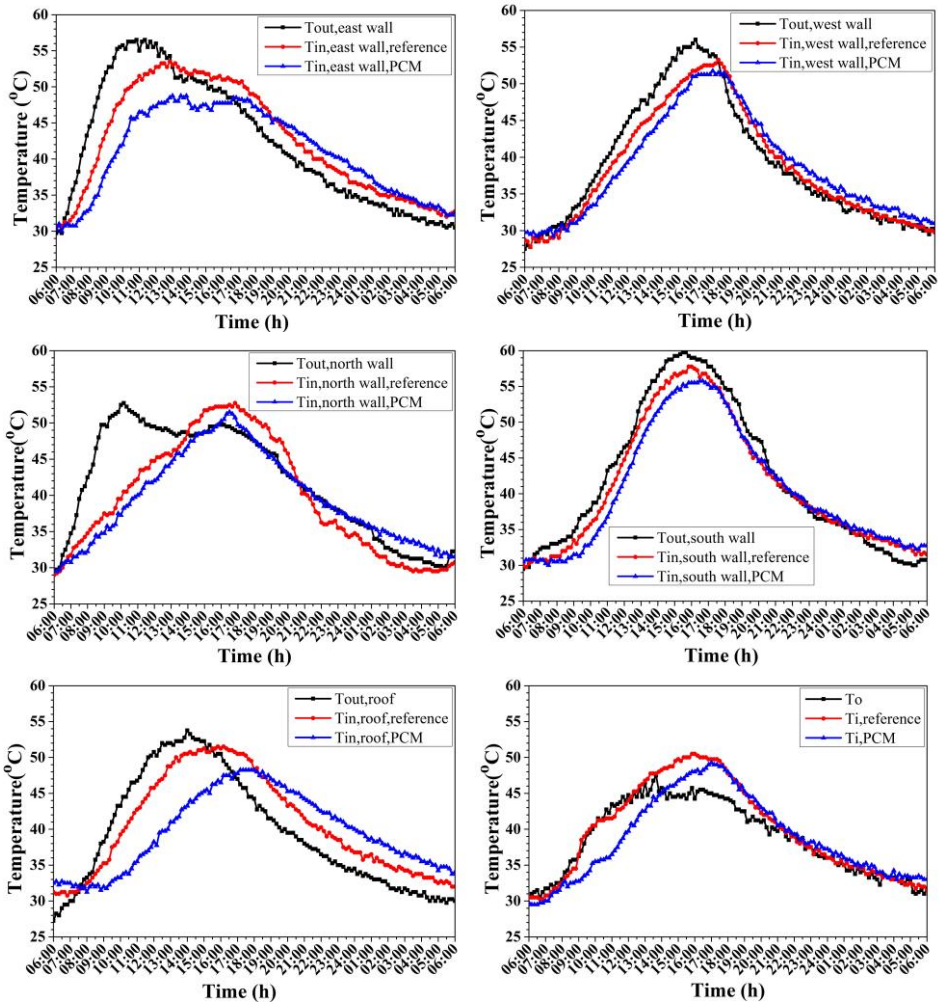

Fig. 5. T_{in}, T_{out} and T_i variation of PCM and reference rooms

A summary of the results obtained for this case is shown in Table 6.

Table 6. Summary of experimental results obtained in the current study

Element	MTR (°C)	ATFR (°C)	DF (%)	TL (min)	MHGR (%)
East wall	2.75	2.4	12.8	40	9.3
West wall	1.25	2.3	11.7	20	4.4
North wall	1.5	3.3	12.5	20	2.7
South wall	2.25	2.1	13.3	30	6.7
Roof	3.25	6.5	25.6	70	11.8

3.4.2. Hourly analysis of PCM room thermal performance

The experimental work was conducted on a hot summer day, 15 September 2022. Fig. 6 shows the T_{in} and T_i for roofs and walls of the reference and PCM rooms against T_o and SR. Table 7 summarises the main average results obtained in this study.

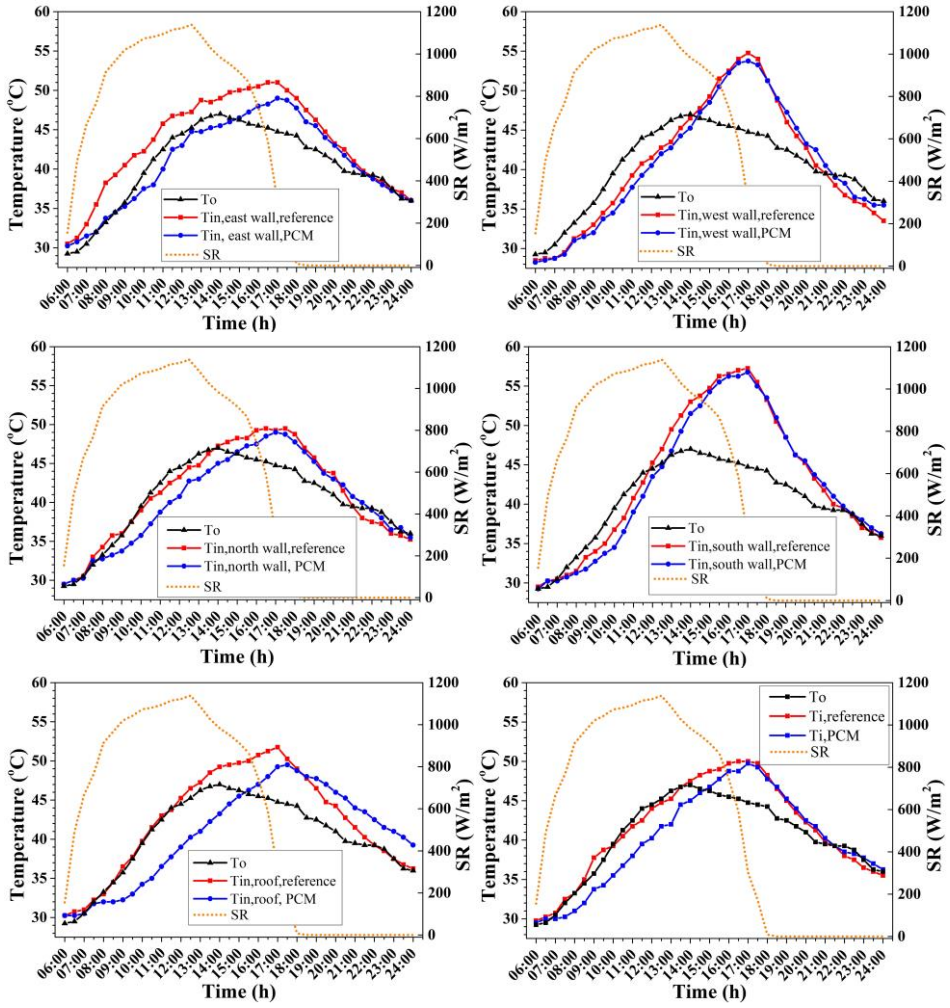

Fig. 6. T_{in} and T_i variation of reference and PCM rooms

Table 7. Summary results for the PCM compared with the reference elements

Element	Average MTD (°C)	Average HTR (%)	Average HHGR (%)
East wall	1.69	4.9	16.9
West wall	1.67	4.6	5.4
North wall	0.71	1.8	9.8
South wall	0.98	2.3	6.2
Roof	3.63	8.2	18.9

3.4.3. Monthly numerical investigation of PCM room thermal performance

The experimental results obtained earlier have been extended numerically to show the PCM thermal performance over a long-term summer period. The numerical studies were conducted for six months (May to October 2021). The room model in numerical studies was verified against the experimental results showing good agreement considering the room indoor air temperature with a maximum difference of 6.1% and 7.9% observed between the experimental and simulation curves of the reference and PCM rooms, respectively. The PCM contribution to the room was quantified for the monthly hottest days. Fig. 7 shows the average indoor temperature of reference and PCM rooms.

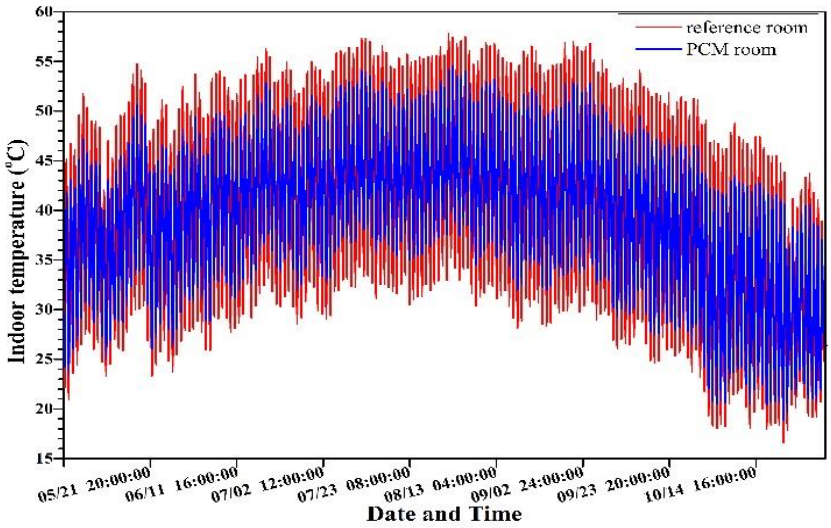

Fig. 7. Hourly indoor temperature variation of reference and PCM rooms

Table 8 lists the average results of indicators analysed in this study.

Table 8. Summary of study findings

Month	ATFR (°C)	TLLR (%)	Total AHGR (%)	CO_2ES (kg CO_2/day)	ECS (IQD/day)
May	5.89	53.83	169.84	2.21	244.6
Jun	5.70	41.69	172.92	2.25	249
Jul	5.02	38.04	165.39	2.16	238.2
Aug	5.05	37.63	173.96	2.27	250.5
Sept	5.95	45.01	169.07	2.21	243.5
Oct	5.88	37.37	146.14	1.91	210.4

3.5. Performance of PCM room-combined thermal insulation

This numerical study considered traditional expanded polystyrene (EPS) thermal insulation to be applied to the PCM room with different thicknesses.

The optimal position of the EPS layer involved was specified first, and then the optimal EPS thickness was analysed at that best position. In general, the cases where the EPS layer was placed near the indoor environment (EPS-i and EPS-m) showed better PCM liquid fraction evolution than the case where the EPS layer was placed outside (EPS-o). The simulation was performed for the reference room model compared with the room with PCM only and PCM combined with EPS of 0.5, 1, 1.5 and 2 cm thicknesses. Table 9 summarises the results of the above cases.

Table 9. Summary of results obtained for modified rooms

Month	RMTR (%)				TL (min)					ATFR (°C)					OTR (%)					AHGR (%)			
	PCM-EPS(0.5)	PCM-EPS(1)	PCM-EPS(1.5)	PCM-EPS(2)	PCM	PCM-EPS(0.5)	PCM-EPS(1)	PCM-EPS(1.5)	PCM-EPS(2)	PCM	PCM-EPS(0.5)	PCM-EPS(1)	PCM-EPS(1.5)	PCM-EPS(2)	PCM	PCM-EPS(0.5)	PCM-EPS(1)	PCM-EPS(1.5)	PCM-EPS(2)	PCM-EPS(0.5)	PCM-EPS(1)	PCM-EPS(1.5)	PCM-EPS(2)
May	45.1	83.4	112.2	133.9	62.7	112	151.3	174.7	191.3	5.5	6.9	7.1	6.8	6.4	5.1	7.5	8.2	8.4	8.5	46.3	72.8	86.4	93.8
Jun	56.4	94.9	121.5	141.3	67.3	99.3	128	146	160.7	4.8	6.3	6.5	6.2	5.8	4.8	6.9	7.3	7.3	7.1	41.1	69.2	76.1	82.5
Jul	65.6	107.4	135.9	156.3	68	102.7	130.7	147.3	158.7	3.9	5.2	5.2	4.9	4.4	3.9	5.8	6.2	6.1	5.9	43.5	65.5	75.9	80.9
Aug	59.4	97.2	124.4	143.2	63.3	99.3	124.7	142.7	155.3	3.9	5.5	5.7	5.4	4.9	3.7	5.5	5.9	5.9	5.7	50.4	75.3	87.7	98.6
Sep	53.2	92.8	120.5	138.9	51.3	95.3	122	142	157.3	5.1	6.6	6.7	6.4	5.9	4.3	6.3	6.6	6.4	6.0	53.8	80.7	93.3	99.3
Oct	55.4	97.9	125.2	144.4	48	97.3	142.7	168.7	189.3	4.6	7.1	8.2	8.5	8.6	3.5	6.8	8.0	8.4	8.4	71.3	122.1	150.8	167.7

3.6. Effect of natural night ventilation on the indoor thermal comfort

The role of NNV was studied considering the improvement in the indoor temperature due to the NNV period, window orientation and role of WWR.

3.6.1. Effect of NNV period on the indoor thermal comfort

The effect of the NNV period on indoor thermal comfort was investigated experimentally through opened windows for 1-6 hours. The experiments were performed from the 18th to the 23rd of September 2021. Windows of reference and PCM rooms were kept open for one hour from 18:00 to 19:00 on 18.09.2021, for two hours from 18:00 to 20:00 on 19.09.2021, and up to six hours from 18:00 to 00:00 on 23.09.2021, as indicated in Fig. 8.

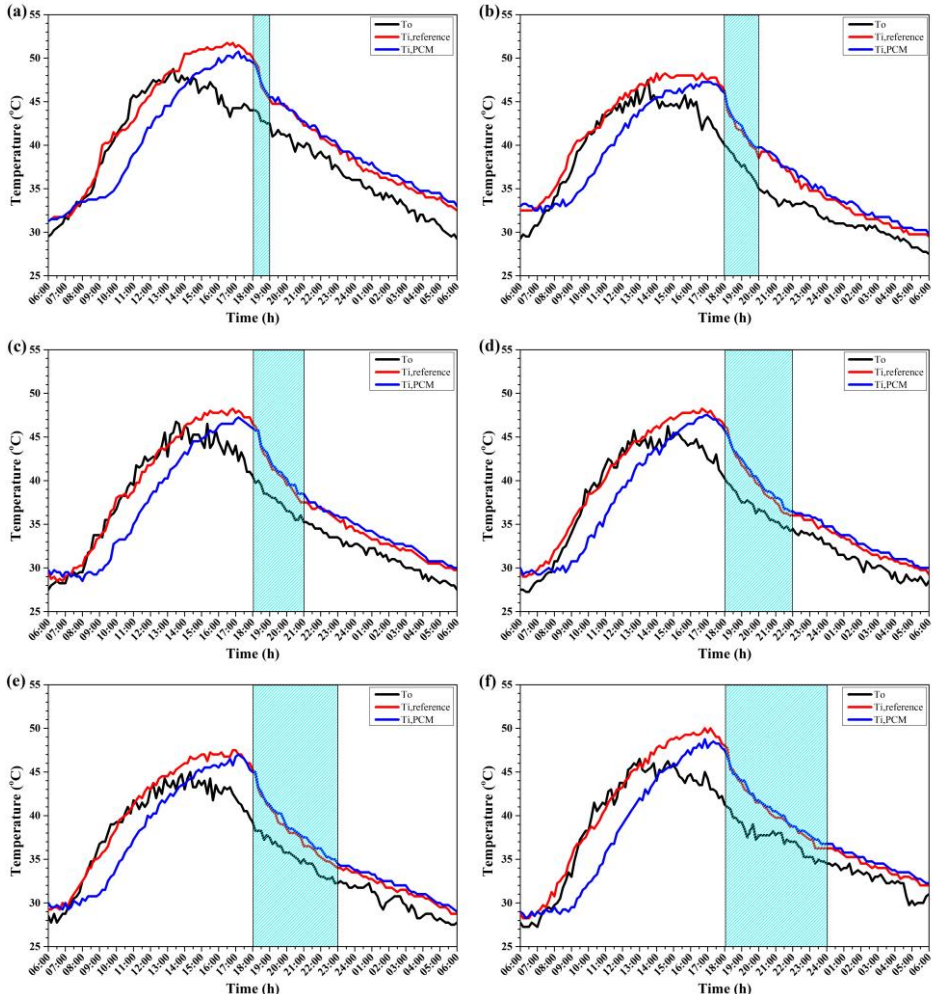

Fig. 8. T_i and T_o of reference and PCM rooms over the NNV periods

The average indoor temperature reduction (AITR) during the last six hours of each thermal cycle (i.e., from 00:00 to 6:00) was considered to study the effect of every NNV period on the temperature variation of the next cycle. Although the indoor temperature of the PCM room is still higher than that of the reference room in the night period, a positive enhancement can be noticed in both rooms when NNV is applied. However, this enhancement was relatively slight regardless of the NNV period due to the high outside ambient temperature at night compared with the indoor temperature of the room and the dependency on the buoyancy forces to transfer the heat through the window (natural ventilation). The temperature difference in the 1st, 2nd, 3rd, 4th, 5th and 6th cycle was 0.632 °C, 0.555 °C, 0.493 °C, 0.451 °C, 0.444 °C and 0.438 °C, respectively. These values are equivalent to AITR in the PCM room

by 12.2%, 21.9%, 28.6%, 29.7% and 30.7%, respectively, when 2 hrs, 3 hrs, 4 hrs, 5 hrs and 6 hrs of NNV are applied compared with 1 hr NNV. This reveals that applying NNV for 4, 5, and 6 hours has nearly the exact indoor temperature enhancement percentages. Considering the OT concept, the maximum OTR has increased inconsistently from 6:00 to 12:00, achieving 12.8%, 11.74%, 12%, 12.45%, 11.2% and 15.2%, respectively, in the 1st, 2nd, 3rd, 4th, 5th and 6th day-cycle. These OTR values indicate no influence of NNV on the OT of the PCM room in the next cycle compared with the reference room, which was more affected by the outdoor ambient temperature and solar radiation during the day.

3.6.2. Effect of window orientation

The effect of window direction compared with the reference case, east direction (E), was studied numerically considering the other three wall directions; south (S), west (W) and north (N). The other orientations are also studied by rotating the room 45° clockwise (i.e. north-east (NE), south-east (SE), south-west (SW) and north-west (NW). The NNV was applied for six hours, starting from 18:00 to 24:00, over the simulation period of six summer months.

According to the numerical results, the NNV through a single-sided window could not improve the indoor temperature of the PCM room by more than 1 °C during May-September, regardless of window orientation. This is attributed to the high outdoor air temperature at night, which was insufficient to release heat from the PCM room considering the wind speed only. The trend differed in October, where the S and SW orientations showed better AITR than the other orientations by more than 1.2 °C.

In summary, the non-ventilated PCM room could be enhanced during hot months (May to September) by an average AITR of 0.51 °C 0.52 °C, 0.68 °C, 0.64 °C, 0.65 °C, 0.68 °C, 0.88 °C and 0.89 °C at the N, NE, E, SE, S, SW, W and NW orientations, respectively. Besides, in comparison to E orientation, only the W and NW orientations could improve the indoor thermal comfort over the PCM room with an E-oriented window by 29.3% and 31.1%, respectively.

3.6.3. Effect of Window-to-wall ratio

The WWR was analysed considering WWR10, WWR12, WWR14, WWR16, 18 WWR and 20 WWR compared with the reference case of 8.75 WWR for the PCM room with NW orientation, the best case obtained in subsection 4.6.2. The effect of WWR on indoor thermal comfort was analysed

considering the AITR of the PCM room with NNV at different WWRs compared with the PCM room with no ventilation.

The AITR of the PCM room decreased as the WWR increased during the simulated period, indicating better thermal comfort. However, the influence of WWR was relatively similar during all months, except during May and October, which showed better AITR influenced by the colder nights. In an average of all months, the AITR of the PCM room was enhanced by 0.89 °C at WWR=8.75%, 0.92 °C at WWR=10%, 0.97 °C at WWR=12%, 1.01 °C at WWR=14%, 1.05 °C at WWR=16%, 1.09 °C at WWR=18% and 1.14 °C at WWR=20%. These AITR values are equivalent to 3.2%, 8.4%, 13.5%, 18.1%, 22.9% and 27.5% at WWR of 10%, 12%, 14%, 16%, 18% and 20%, respectively, compared with the reference case of WWR=8.75%.

The above results showed that applying NNV for 6 h at the best window orientation (NW) and WWR (20%) could reduce the PCM room indoor temperature by only 1.14 °C over the case of a non-ventilated PCM room directed towards NW. This temperature reduction is too slight compared to the heat released from the PCM at night. Therefore, applying forced NV is suggested for such harsh weather locations considering the ventilation time and amount of ventilated air. Besides, an alternative cooling medium could be processed to expedite the PCM solidification phase.

4. NEW SCIENTIFIC RESULTS

This section presents the new scientific findings from the research as follows:

1. Effect of phase change material position on the roof's thermal performance

I have pointed out that the optimal position of phase change material (PCM) strongly influences the roof's thermal performance from both energetic and thermal comfort viewpoints. Besides, I proved experimentally that the PCM was more beneficial as the outer surface temperature increased.

Based on the experimental findings, I found that positioning the PCM layer near the outer roof side (between the roofing and main layers) has reduced the inner surface temperature and indoor ambient temperature regardless of the roof's outer surface temperature at non-ventilated conditions. Besides, positioning the PCM layer in the middle of a composite roof could enhance the indoor thermal comfort superior to the position near the inner roof layer (near indoor).

Compared with the roof without PCM, I proved that the PCM layer at the outside position had reduced the maximum indoor temperature by 12.9%, along with average indoor temperature fluctuation reduction by 9 °C during the thermal cycle and time delay by 140-180 min. At the highest outer surface temperatures, the roof's inner surface temperature decreased as the PCM layer moved from the inner towards the outer position by 36.5%, 66.3% and 74.8%.

2. Effect of phase change material thickness on roof's thermal performance

I experimentally investigated the optimal thickness of the PCM layer incorporated in a roof and its effect on thermal performance. I found that increasing PCM layer thickness from 1 cm to 1.5 and 2 cm has increased the roof's thermal performance and improved indoor thermal comfort. In this regard, the PCM layer thickness of 2 mm has reduced the maximum indoor temperature by about 13.9% and extended the temperature time lag by 240-270 min compared with the roof without PCM. However, I found that increasing PCM layer thickness has descending effectiveness in which increasing thickness from 1 to 1.5 cm has reduced the indoor temperature by 20.5% while increasing the thickness from 1.5 to 2 cm has reduced it by about 3% only.

I noticed that increasing PCM layer thickness "x" by 0.5 cm has enhanced the roof thermal resistance in terms of the decrement factor "y" according to the linear equation:

$$y = -0.1x + 0.6367 \qquad R^2 = 0.9868$$

I observed that increasing PCM thickness in the non-ventilated roof has limited advantages in passive applications due to the poor PCM solidification

phase at night. According to the experimental results, I found that the average temperature fluctuation reduction at 2 cm PCM layer thickness had poorer thermal performance than 1.5 cm thickness, considering the full thermal cycle. I discovered that the PCM layer of 1.5 cm could reduce the indoor temperature fluctuations by an average of 10.04 °C compared with the bare roof. In contrast, 1 and 2 cm PCM thicknesses could reduce the fluctuations by 8.13 °C and 9.75 °C, respectively

3. The influence of encapsulation heat transfer area on bricks-based PCM

I have examined and justified the effect of encapsulation area on the PCM thermal performance when immersed into concrete bricks. I have proven that in passive novel bricks containing PCM capsules with different shapes and sizes, the overall heat transfer encapsulation area was the main influential parameter of PCM performance during the thermal cycle since the same PCM quantity was involved.

Based on the experimental results, I observed that concrete bricks with many PCM capsules had lower inner surface temperatures than those based on bulky PCM capsules, thanks to the high PCM heat transfer area. However, although increased encapsulation area has improved the melting/solidification phases, I noticed that increasing encapsulation area was critical and excessive area could reach a fast melting phase and decline heat storage early regardless of the capsules' shape.

I found that 320 cm2 overall heat transfer area was the best for ~45g PCM in the concrete brick, reducing the maximum inner surface temperature by ~1.88 °C and lagging peak temperature by 42.5 min on average. Technically, the mechanical strength of this PCM brick type declined by 28.2% compared with the reference one.

4. Thermal comfort and energetic evaluation of scaled PCM room

I assessed the contribution of PCM to the indoor thermal comfort and energy saving of a scaled room under no ventilation compared with a reference room. I showed that the PCM had improved indoor thermal comfort and energy saving remarkably during day hours. According to experimental results, I showed that the maximum indoor temperature has decreased by up to 5.75 °C in the PCM room compared to the reference room. From the energetic viewpoint, I found that the PCM effectiveness during the day is time-dependent with respect to the sun's position. Considering walls, the east-oriented wall performed better in the first half of the day, whereas the west-oriented wall performed well in the afternoon. The maximum temperature reduction of the east wall reached 2.75 °C, whereas the west wall showed a 2.25 °C temperature reduction. Besides, all PCM walls showed roughly

similar decrement factor of 11.7%-13.3% compared with the reference walls. I confirmed that the roof was the most effective element in the room, responsible for an average surface temperature reduction of 3.25 °C, a decrement factor of 25.6% and a total heat gain reduction of 35%-40% over the reference roof.

Based on the hourly analysis, I noticed that the best effectiveness hour for the PCM room is at 9:00, in which the indoor temperature reduction "y" after this hour was linearly declined with time "x", according to the following equation:

$$y = -29.12x + 22.16 \qquad R^2 = 0.9664$$

Energetically, I had seen that the PCM was most effective during the first half of the day, particularly from 9:00 to 11:00, more than the rest day hours. Besides, the PCM involved in walls should vary, considering their orientation and period of exposure to solar radiation.

Considering the long-term numerical analysis, I observed that the average indoor temperature fluctuations were minimised during summer by up to 6 °C in the PCM room compared to the reference room. Moreover, I found that the thermal load levelling during the thermal cycle was reduced by 38%-59%, with superior performance observed in May and lower in October. From the energetic standpoint, I showed that the average heat gain reduction during the hottest summer months ranged between 66.6%- 76.5%. Accordingly, I estimated that the PCM incorporated could save CO_2 emission by up to 2.27 kg CO_2/day and electricity by up to 250 IQD/day.

5. Effect of thermal insulation with PCM room

I investigated the optimal thickness of the EPS layer (0.5, 1, 1.5 and 2 cm) installed in the PCM room at the optimal position. I proved that increasing EPS layer thickness had improved the thermal performance of the PCM room noticeably from the energetic and thermal comfort perception. However, I observed that increasing EPS layer thickness is limited when considering the full thermal cycle and had adverse behaviour under a non-conditioned PCM room. On average summer months, I disclosed that installing EPS with 0.5, 1, 1.5 and 2 cm layer thickness had increased the maximum indoor temperature reduction over the PCM room by 55.7%, 95.4%, 123.1% and 142.8%, respectively.

I evidenced that the average temperature fluctuation during May-September was reduced by up to 35% when installing a 1 cm thickness of EPS with the PCM room, compared with only 20% when 2 cm was installed. I also exhibited that the thicker EPS layer than 1 cm installed in the PCM room has

performed poorly compared with that of EPS layer thickness equal to/or lower than 1 cm during June-September.

From the energetic viewpoint, I showed that the envelope total heat gain reduction "y" linearly increases with the increased EPS layer thickness by 0.5 mm "x", according to the following positive relationship:

$$y = 34.46x + 39.65 \qquad R^2 = 0.9273$$

6. Role of natural night ventilation to enhance thermal comfort of PCM room

I explored the role of natural night ventilation (NNV) experimentally through a single-side window to enhance the PCM room thermal comfort. I showed that increasing the NNV period from 1 h to 6 h could slightly decrease the PCM room temperature compared to that of the reference room. I observed that increasing the NNV period to 4 h has narrowed the indoor temperature difference between PCM and reference rooms noticeably, according to the following linear equation. However, a slight temperature difference was attained at 5 and 6 h.

$$y = -0.0604x + 0.684 \qquad R^2 = 0.9836$$

I also revealed that the daily maximum operative temperature in the PCM room was inconsistently increased by 11.2%-12.8% in the first half of the next day, indicating no influence of the NNV on the following thermal cycle.

Considering the window orientation, I proved that the NNV could improve the thermal performance of the PCM room further when directing the room towards the north-west direction. At this orientation, the indoor temperature of the PCM room has decreased by 1.2 °C at night compared with the PCM room without NV.

I also investigated the effect of NNV through an enlarged window-to-wall ratio (WWR) from 10% to 20% with a 2% increment factor on the PCM room indoor temperature. At the north-west room orientation, I disclosed a positive linear relationship between increasing WWR "x" and decreasing the indoor temperature of PCM room "y", according to the following equation:

$$y = 2.4229x + 20.743 \qquad R^2 = 0.9994$$

Considering the above statements, I improved the average indoor thermal comfort of the PCM room by about 27.5% when enlarging WWR from 8.75% (reference WWR) to 20% during summer.

5. CONCLUSION AND SUGGESTIONS

The performance of phase change material (PCM) incorporated into a building envelope has been investigated experimentally and numerically under hot location. Based on the results, the following conclusions can be drawn:

- Positioning the PCM layer near the outdoor edge of the roof performed better than the position in the middle or near the indoor zone. Besides, increasing PCM layer thickness in the roof from 1 cm to 1.5 and 2 cm has increased the PCM effectiveness. However, adverse PCM thermal behaviour was observed at night for 2 cm PCM layer thickness.
- The overall heat transfer area is the main influential parameter on the thermal performance of PCM bricks regardless of the shape of the capsules. Immersed many PCM capsules into concrete bricks had better thermal performance than bulky containers. The mechanical strength of PCM brick declined compared with the bare brick by about 28%.
- The PCM effectiveness is time-dependent, where the PCM elements exposed to solar radiation for a long time are more beneficial than their corresponding ones. Energy saving of up to 40% could be attained through the roof than walls. Moreover, the indoor temperature of the PCM room was stabilised, shaved and shifted considerably.
- The thermal insulation could maximise PCM's effectiveness and achieve further energy saving. However, the position and thickness of the thermal insulation should be studied properly to ensure no influence on the PCM melting/solidification phases. It was found that positioning 1 cm of insulation next to the PCM layer from the indoor side is optimal.
- Utilising NNV through a single-side window could slightly improve the indoor temperature during night hours due to high outdoor temperatures. NNV for 4 h was critical to reduce the PCM room indoor temperature, in which a slight improvement was observed with 5 and 6 h. The window orientation has affected the thermal comfort, and the orientation towards the north-west direction is the best. Besides, the higher window-to-wall ratio (WWR) resulted in better PCM room thermal comfort.

The scope of this work could be extended to consider the PCM incorporation with transparent elements (i.e., windows), which have an essential influence on the built environment in hot locations. The PCM effectiveness under real conditions, involving the impact of occupants and equipment under controlled conditions (mechanical ventilation), is extremely advised. PCM-coupled solar thermal system for space heating has many research gaps need to be addressed. Besides, the PCM contribution to cooling and heating load reduction is suggested considering composite PCM layers with different melting temperatures. Finally, the study of real buildings considering the economic and environmental aspects is also crucial to foretell the technology feasibility.

6. SUMMARY

INCORPORATION OF PHASE CHANGE MATERIAL INTO BUILDING ENVELOPE UNDER HOT LOCATION

Experimental and numerical investigations have been conducted to evaluate the thermal performance of phase change material (PCM) incorporated into the building envelope under severe hot conditions. Therefore, two rooms were built and examined in-site, one passively incorporated with PCM into the roof and walls (PCM room) and another without PCM. The optimal PCM position and thickness into the roof were considered in the PCM room, along with the best thermally-performed PCM brick. Numerical studies have been verified on a validated model to investigate the PCM effectiveness over the summer months. Furthermore, the role of thermal insulation at different positions and thicknesses was investigated along with the effect of natural night ventilation (NNV) at different periods, window orientation and window-to-wall ratio (WWR).

The experimental and numerical results indicated notable effectiveness of PCM under severe hot summer conditions. The PCM layer was better positioned near the outdoor environment where the melting and solidification phases were guaranteed. Besides, increased PCM layer thickness in the roof had well thermal advantages. However, the thicker PCM layer showed poor thermal performance during solidification. Considering the PCM bricks, the PCM involved in capsules performed better than bulky PCM capsules due to the enlarged heat transfer area. However, the mechanical strength of the PCM brick declined compared to that of the reference brick.

The PCM room generally showed better thermal comfort and energy saving than the reference room. Experimental and numerical studies showed that the roof performed much better than the walls due to long-time exposure to solar radiation and the PCM quantity incorporated. Besides, the walls that experienced high solar radiation performed better than the others.

Numerical studies showed that installing insulation with the PCM is beneficial to enhance building performance. It was shown that positioning the thermal insulation next to the PCM layer from the indoor side is optimal. Besides, the insulation layer of 1 cm was better than thicker layers during the thermal cycle. Experimental and numerical investigations showed that the NNV could slightly enhance the indoor temperature regardless of the NNV period. Besides, the NNV through a single-side window could reduce the temperature by about one degree at the best window orientation and size concerning the non-ventilated case.

7. MOST IMPORTANT PUBLICATIONS RELATED TO THE THESIS

Refereed papers in foreign languages:

1. Al-Yasiri, Q., Szabó, M. (2021): Incorporation of phase change materials into building envelope for thermal comfort and energy saving: A comprehensive analysis, Journal of Building Engineering, Vol. 36, pp. 102122. https://doi.org/10.1016/j.jobe.2020.102122 (Scopus: Q1/D1, IF: 7.144).
2. Al-Yasiri, Q., Szabó, M. (2021): Experimental evaluation of the optimal position of a macroencapsulated phase change material incorporated composite roof under hot climate conditions, Sustainable Energy Technologies and Assessments, Vol. 45, pp. 101121. https://doi.org/10.1016/j.seta.2021.101121 (Scopus: Q1, IF: 7,632).
3. Al-Yasiri, Q., Szabó, M. (2021): Case study on the optimal thickness of phase change material incorporated composite roof under hot climate conditions, Case Studies in Construction Materials, Vol. 14, pp. e00522. https://doi.org/10.1016/j.cscm.2021.e00522 (Scopus: Q1, IF: 4.934).
4. Al-Yasiri, Q., Szabó, M. (2021): Thermal performance of concrete bricks based phase change material encapsulated by various aluminium containers: An experimental study under Iraqi hot climate conditions, Journal of Energy Storage, Vol. 40, pp. 102710. https://doi.org/10.1016/j.est.2021.102710 (Scopus: Q1, IF: 8.907).
5. Al-Yasiri, Q., Szabó, M. (2022): Energetic and thermal comfort assessment of phase change material passively incorporated building envelope in severe hot climate: An experimental study, Applied Energy, Vol. 314, pp. 118957. https://doi.org/10.1016/j.apenergy.2022.118957 (Scopus: Q1/D1, IF: 11.446).
6. Al-Yasiri, Q., Szabó, M. (2022): Phase change material coupled building envelope for thermal comfort and energy-saving: Effect of natural night ventilation under hot climate, Journal of Cleaner Production, Vol. 365, pp. 132839. https://doi.org/10.1016/j.jclepro.2022.132839 (Scopus: Q1/D1, IF: 11.072).
7. Al-Yasiri, Q., Szabó, M. (2023): Experimental study of PCM-enhanced building envelope towards energy-saving and decarbonisation in a severe hot climate, Energy and Buildings, Vol. 279, pp. 112680. https://doi.org/10.1016/j.enbuild.2022.112680 (Scopus:Q1/D1,IF: 7.201).
8. Al-Yasiri, Q., Szabó, M. (2023): Numerical analysis of thin building envelope-integrated phase change material towards energy-efficient buildings in a severely hot location, Sustainable Cities and Society, Vol. 89, pp. 104365. https://doi.org/10.1016/j.scs.2022.104365 (Scopus: Q1/D1, IF: 10.696).